



## Estimates of mean signal offsets

Ing.Dr.Stanislav Sykora, February 06, 2003

This Note describes the algorithms used by the Stelar AcqNmr software to estimate the *mean Larmor frequency offset* and the *receiver phase* from a noisy FID signal.

### Theoretical

For the purpose of this discussion we shall view the evolution of an FID in the complex Cartesian plane (Fig.1.), making the X-axis coordinate correspond to the quad-receiver's in-phase signal (channel A) and the Y-axis coordinate to the out-of-phase signal (channel B).

This corresponds to the DISPA (dispersion-absorption) plots used occasionally in ESR and NMR spectroscopies, except for the fact that the curve parameter is time rather than frequency. Consequently, it seems appropriate to call such plots **tDISPA** (time-domain DISPA).

The tDISPA plot of a noiseless FID of a sample with just one spectral component is a spiral line. Just after the RF pulse, the ideal signal corresponds to the point on the red spiral which has the largest radius. As time evolves, the signal moves along the spiral, obeying two rules:

**i)** Its argument  $\phi(t)$  varies linearly with time  $t$  at a rate  $\omega$  (angular velocity) which matches the signal's frequency offset  $\omega = \omega_L - \omega_{ref}$ , i.e., the difference between Larmor frequency  $\omega_L$  and the receiver reference frequency  $\omega_{ref}$ . This parameter may be either positive or negative, giving rise to counter-clockwise or clockwise rotating spiral traces, respectively. In the on-resonance condition,  $\omega$  is null and the spiral trace degenerates to a straight line joining the starting point with the origin.

**ii)** Its radius  $r(t)$  decays, following the approximate exponential rule  $r = r_0 \exp(-t/T_2^*)$ .

When the sample contains more than one spectral component, the ideal FID trace is more complex since the components  $r(t)$  and  $\phi(t)$  are both modulated in a more or less complex way. Even in this case, however, the following statements hold:

- 1) The *starting value of the derivative*  $\phi'(0)$  equals the *mean signal offset* (or, in spectroscopic terms, the *first spectral moment*).
- 2) The *mean value of*  $\phi'(t)$  over the whole FID also equals the *mean signal offset*.
- 3) The *starting value*  $\Omega = \phi(0)$  is the *receiver phase* (common for all spectral components).

What makes the tDISPA plots interesting is that signal offset and receiver-phase affect only the argument  $\phi(t)$  and not the radius  $r(t)$ . This means that any complexities arising from the decay (line shape effects) are neatly removed. In order to evaluate the *mean signal offset* and the *receiver phase* from the FID, one needs to concentrate on  $\phi(t)$  only.

In practice, there is no way to measure the ideal FID since it is always partially corrupted by *signal noise*. The best we can get is a set of data points acquired at equidistant time intervals and distributed along the ideal signal-trace spiral. The noise is normally white and homogeneous throughout the Cartesian plane (it does not depend upon signal parameters like magnitude or phase).

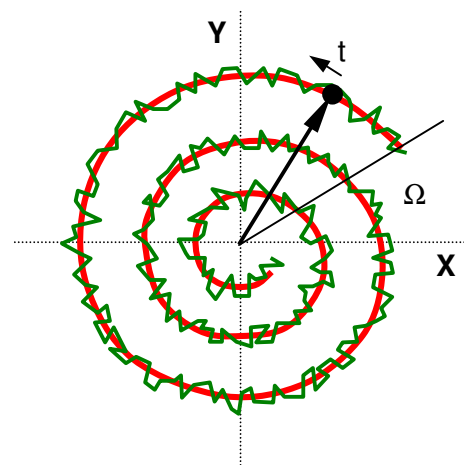


**Figure 1. tDISPA plot of an FID**

The ideal signal (red) is not experimentally accessible because of the superposed noise. Experimental data points (corners of the green trace) are distributed randomly around the ideal signal trace. Notice that the noise may occasionally cause local "backtracking" of the experimental trace.

The challenge is to estimate the average linear rate of variation of  $\phi(t)$  and its starting value  $\Omega$  in the presence of noise. The first approach, implemented in the AcqNmr software up to version 2.0, consisted of four steps:

### Algorithm A

#### A1. Data window selection.

It is non advisable to use all points of an FID since

- a) the first few points are sometimes contaminated by dead-time and probe-ringing artifacts and
- b) the points in the tailing section of an FID may contain too little signal.

The offset-estimate algorithm therefore uses an FID "data window" defined by the User-settable first-point and last-point indices (parameters EWIP and EWEP, respectively).

#### A2. Estimate of the mean rate of variation of $\phi(t)$ throughout the specified window.

This is not as elementary as it sounds. The data points  $P_k(t_k) = [x_k, y_k]$  are acquired and stored as two arrays of values  $\{x_k\}$  and  $\{y_k\}$ . The corresponding times  $\{t_k\}$  can be easily and precisely computed using acquisition delay (ACQD) and dwell-time (DW) parameters.

The problem is that, given a data point  $P_k$ , one can only estimate its phase  $\phi_k$  (the argument of  $P_k$ ) *modulo*  $2\pi$ . In other words, given a single point  $P_k$  in the tDISPA diagram, we can't know how many times the FID spiral to which it belongs has already circled around the origin.

To overcome this drawback, *one must follow the data points one-by-one and sum up (accumulate) the phase argument differences between the consecutive ones*<sup>1</sup>. Only then can the average  $\omega$  be computed, dividing the sum of argument differences by the total elapsed time.

#### A3. Estimate of the receiver phase $\Omega$ .

The value of  $\Omega = \phi(0)$  is computed as the *argument of the first data point* corrected for its acquisition delay (the correction uses the mean offset estimated in the preceding step). Since this makes  $\Omega$  resent directly the noise error associated with the first data point (no averaging), we have never considered the receiver phase estimate to be particularly reliable, unless the data had a very good signal-to-noise ratio and were acquired close to resonance.

#### A4. Multi-block experiments averaging.

In multi-block experiments, the above estimates of  $\omega$  and  $\Omega$  are carried out separately for each block. The mean value of both entities is then determined as a simple arithmetic average of the partial estimates.

### Problems

Algorithm (A) worked quite well for data sets with good signal-to-noise ratios (S/N) and has been incorporated into automated procedures for acquisition of  $T_1$  relaxation profiles. However, it turned out to be *unreliable in situations characterized by S/N smaller than about 5*. Even more serious was the fact that in multi-block experiments, the presence of a *single block* with low S/N often lead to a wrong offset correction and thus ruined an automated profile acquisition. With low S/N samples, such situations are common even in the basic sequences (first blocks of PP/S, last block of NP/S) and they are unavoidable in those sequences in which the signal crosses zero at some tau-value (IR/S).

In order to understand better what happens at low S/N ratios, consider Fig.2. Passing from the ideal FID signal to an experimental one, each signal point in the tDISPA plot can be characterized by an *expected error ellipsoid*. Since the signal noise is equal in both channels (unless there is a hardware problem), the ellipsoid is actually an *expected error disk of constant radius*, moving along the ideal signal spiral (Fig.2a). It is evident that the process of estimating the phase increment between two consecutive data points becomes unreliable whenever the error disk gets close to the origin (Fig.2b) or, even worse, encircles the

<sup>1</sup> The algorithm uses a closed-form formula for the phase difference  $\Delta_k$  between points  $[x_k, y_k]$  and  $[x_{k+1}, y_{k+1}]$ . Unless the data are severely undersampled, these never exceed  $\pi$ .

origin. We then enter the situation in which the phase-increment formula may supply wrong results due to the uncertainty between  $\alpha$  and  $2\pi-\alpha$  (Fig.2c).

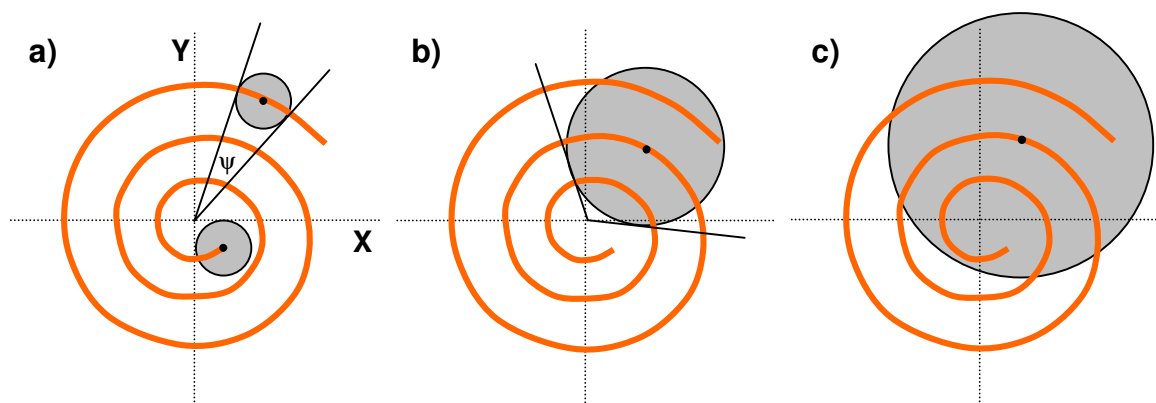


**Figure 2. tDISPA plots of FID's with error disks**

**a)** Examples of expected-error disks in the case of relatively good S/N ratio. The center of the disk moves along the ideal-signal trace (red) while the radius of the disk remains constant. The experimental data point corresponding to the ideal one (black dot) is expected to fall off with a probability corresponding to the 2D Gaussian distribution centered at the ideal data point whose *probable* deviation matches the radius of the error disk. The *error-disk viewing angle*  $\psi$  is defined as shown (notice that, unlike the disk radius, it is not constant but increases during the signal evolution).

**b)** An intermediate case with S/N ratio of a bit less than 2. Once the signal has partially decayed, the error disk gets so close to the origin that phase angles between consecutive could easily become greater than  $\pi$  in which case angle-estimates might fail by  $2\pi$ . This is a border-case, with the initial portions of the FID probably still good for a reliable offset estimate but the later portions decidedly unsuitable for the task.

**c)** A case with still lower S/N ratio. In a case like this, estimates of phase increments between consecutive data points are quite unreliable and the FID can not be used to determine the offset. The challenge is to make sure that the algorithm shall "recognize" the situation and reject the data rather than computing a nonsensical offset value.

Consequently, Algorithm A had to be modified.

The idea is to *monitor the probable value of the viewing angle  $\psi$  of the error disk and stop accumulating the phase increments as soon as it becomes greater than a predefined limit*. In addition, if the FID data window does not contain a sufficiently large number of *valid* consecutive data pairs, the algorithm *refrains from estimating the offset* and flags the FID as unsuitable for that purpose. Such FID's are then *excluded from any further evaluation* so that, for example, automatic offset corrections are skipped when the data are not good enough to make it reliable.

The new version (algorithm **B**) which shall now be described is deployed in all AcqNmr packages starting from Version 2.0 (all builds).

## Algorithm B

### B1. Data window selection.

The data window selection is done as in Algorithm A. However, the last data point is considered just as a User's global constraint. In practice, the number of considered data points may be much smaller, depending upon the quality of the data (see the next step).

### A2. Estimate of the mean rate of variation of $\phi(t)$ .

The data points are again followed one-by-one and the phase argument differences between the consecutive ones are accumulated. Unlike in Algorithm A, however, the process is interrupted as soon as any of the individual phase differences exceeds a selected threshold value  $\psi_t$  (we use  $\psi_t = \pi/3$ ). The rationale behind this is that a big phase difference between two consecutive data points can happen only if at least one of the following situations occurs:

- noisy data*: the error-disk viewing angle is too large (of the same order of  $\psi_t$ ).
- pathological offset*: the current offset is greater than  $SW \cdot (\psi_t/2\pi)$

In both cases, the offset estimate is classified as unreliable.

Thereafter, if the number  $n$  of accumulated phase increments is at least  $n_t$  (we use  $n_t = 6$ ), we estimate the average  $\omega$  by dividing the accumulated argument differences by the elapsed time. Otherwise, we declare the data insufficient for a reliable offset estimate and terminate.

### **B3.** Estimate of the receiver phase $\Omega$ .

Unlike in Algorithm A, we now use all the valid data points found in the preceding step to estimate the value of  $\Omega = \phi(0)$ . This kind of averaging makes  $\Omega$  much less dependent upon signal noise and thus much more reliable than before.

### **B4.** Multi-block experiments averaging.

As before, in multi-block experiments the above estimates of  $\omega$  and  $\Omega$  are carried out separately for each block. The mean value of both entities is then determined as a *weighed arithmetic average* of the partial estimates. Two extra precautions involved in the process are:

- a) Blocks classified as unreliable in step (B2) are disregarded.
- b) The accepted blocks are weighed according to the total amount of *signal* they contain.

By *signal* we understand in this context the quantity used for further evaluation. For example, when mean data-window magnitudes are used, the *signal* of each block is identified with that quantity. As a result, the blocks with more signal have now a greater weight in the multi-block offset estimate.

## **Conclusions and practical experiences**

Practical tests with different threshold parameters  $\psi_t$  and  $n_t$  were carried out. We have chosen the values which gave the best results in terms of reliability (no unreasonable offset estimates) and sensitivity (good estimates even with low S/N). The chosen values were built directly into the program executable which, in this case, appears preferable to leaving them open as User-settable parameters.

The resulting algorithm seems to be very satisfactory. Reasonable offset estimates are obtained for FID's with S/N ratios as low as 2:1. Around and below that limit, the FID's are become classified as unreliable (for S/N close to 2 this happens just for a few random cases while practically no case passes when S/N is of the order of 1.5 or lower).

As a result, automated measurements with automated offset corrections may be now carried out using any non-CPMG type sequence<sup>2</sup>. Moreover, automation now works fine also on samples with very low S/N ratios.

### **Perspectives**

It is certainly still possible to improve the offset and receiver phase estimates. Since we keep working on new algorithms, keep in touch in order not to miss further improvements and/or new approaches.

---

<sup>2</sup> For CPMG-type sequences, offset estimates and corrections are inhibited.